Purification of the *Escherichia coli* ammonium transporter AmtB reveals a trimeric stoichiometry

Dan BLAKEY*[1], Andrew LEECH†, Gavin H. THOMAS*[2], Graham COUTTS*, Kim FINDLAY‡ and Mike MERRICK*[3]

*Department of Molecular Microbiology, John Innes Centre, Norwich NR4 7UH, U.K., †School of Biological Sciences, University of East Anglia, Norwich NR4 7TJ, U.K., and ‡Department of Cell and Developmental Biology, John Innes Centre, Norwich NR4 7UH, U.K.

The Amt family of high-affinity ammonium transporters is a family of integral membrane proteins that are found in archaea, bacteria, fungi, plants and animals. Furthermore, the family has recently been extended to humans with the recognition that both the erythroid and non-erythroid Rhesus proteins are also ammonium transporters. The *Escherichia coli* AmtB protein offers a good model system for the Amt family and in order to address questions relating to both its structure and function we have overproduced a histidine-tagged form of the protein (AmtB6H) and purified it to homogeneity. We examined the quaternary structure of AmtB6H (which is active *in vivo*) by SDS/PAGE, gel-filtration chromatography, dynamic light scattering and sedimentation ultracentrifugation. The protein was resistant to dissociation by SDS and behaved as a stable oligomer on SDS/PAGE. By equilibrium desorption chromatography we determined the mass ratio of dodecyl β-D-maltoside to AmtB in the detergent-solubilized complex to be 1.03 ± 0.03, and this allowed us to calculate, from analytical-ultracentrifugation data, that AmtB purifies as a trimer.

Key words: ammonium transport, membrane protein, methylammonium permease.

INTRODUCTION

The transport of ammonium across biological membranes is an important physiological process in all domains of life [1]. Genes encoding high-affinity ammonium transporters [methylammonium permease (Mep)/Amt] were first described in *Arabidopsis thaliana* and *Saccharomyces cerevisiae* [2,3], since when more than 50 homologues have been identified. The genes encode highly hydrophobic proteins that are generally between 400 and 450 amino acids in length and which represent a distinct family of transporters found in archaea, bacteria, fungi, plants and animals. The Rhesus (Rh) family of blood antigens also show significant similarity to the Mep/Amt proteins [4] and, by complementation of an *S. cerevisiae* Δ(*mep1*,*2*,*3*) mutant, it has recently been demonstrated that the Rh-associated glycoprotein (RhAG) and the non-erythroid Rh-related glycoprotein (RhCG) can transport ammonium [5]. The recognition of non-erythroid Rh proteins expressed in the kidney, skin and liver, three organs critical for the excretion, secretion and production of ammonia, is also consistent with a physiological function of these proteins in ammonium transport [6].

Escherichia coli AmtB is a 428 amino acid protein with a predicted molecular mass of 44.5 kDa that is encoded by the second gene in the *glnKamtB* operon [7]. It is essential for the transport of methylammonium into the cell and has been shown to complement an *S. cerevisiae* Δ(*mep1*,*2*,*3*) mutant for growth on 1 mM ammonium (G. H. Thomas and A.-M. Marini, unpublished work). The most widely accepted view of the likely mechanism of transport by Amt proteins is that they are secondary transporters that mediate an energy-dependent uptake of the NH_4^+ cation [8]. The bioenergetics of Amt-mediated ammonium transport has been studied in detail in *Corynebacterium glutamicum*, where it was concluded that uptake of (methyl)ammonium was strictly dependent on the membrane potential and that the protein catalyses the uniport of NH_4^+ [9,10]. Very recently, electrophysiological characterization of the LeAMT1;1 ammonium transporter from tomato, following its heterologous expression in *Xenopus* oocytes, has also shown that ammonium transport occurs by uniport of NH_4^+ [11]. A similar mechanism has been proposed for *A. thaliana* AtAMT1;1 [12] and *Synechocystis* [13]. However, these views have been challenged by Soupene et al. [14] who proposed that the Mep/Amt proteins act as ammonium facilitators which serve simply to increase the rate of equilibration of the uncharged species, NH_3, across the cytoplasmic membrane.

While a number of integral membrane secondary transporters have been purified, the tertiary and quaternary structures have been determined for relatively few of these proteins. Nevertheless it is already apparent that not all secondary transporters adopt the same configuration. The lactose transporter, LacS, behaves as if in a monomer–dimer equilibrium [15]. An engineered form of lactose permease, LacY, is a monomer when purified in detergent, although two-dimensional crystals of the protein reveal trimeric complexes [16]. Likewise, the TetA tetracycline transporter also has trigonal symmetry in two-dimensional crystals [17]. By contrast the human erythrocyte anion exchanger (Band 3) and the Na^+/H^+ antiporter, NhaA, crystallize as dimers [18,19]. Genetic studies of the proton-linked multidrug transporter EmrE suggest that it also forms an oligomer *in vivo*, and the recently solved projection structure of this protein, which is predicted to have just four transmembrane helices, reveals an asymmetric dimer [20].

Secondary-structural predictions for members of the Mep/Amt family suggest that they encode membrane proteins with 10–12 transmembrane helices with a C-terminal cytoplasmic extension [2,3,21,22]. The length of this C-terminal domain

Abbreviations used: Mep, methylammonium permease; Rh, Rhesus; RhAG, Rh-associated glycoprotein; DDM, dodecyl β-D-maltoside; IPTG, isopropyl β-D-thiogalactoside; IE, ion-exchange.

[1] Present address: Department of Experimental Psychology, University of Oxford, South Parks Road, Oxford OX1 3UD, U.K.
[2] Present address: Department of Molecular Biology and Biotechnology, University of Sheffield, Sheffield S10 2TN, U.K.
[3] To whom correspondence should be addressed (e-mail mike.merrick@bbsrc.ac.uk).

varies greatly between proteins, in some cases increasing their total length to more than 600 residues (*Caenorhabditis elegans* Amt-3, Swissprot accession no. Q21565, and *Drosophila melanogaster* Amt-1, Swissprot accession no. Q9VFA9). Mep/Amt proteins from *S. cerevisiae* and *A. thaliana* are predicted to contain 11 transmembrane helices, with the N-terminus positioned extracellularly and the C-terminus positioned cytoplasmically, and this is likely to reflect the structure of most Mep/Amt proteins [21,23]. However, the most detailed empirical topological analysis has been carried out with *E. coli* AmtB. *In silico* analysis and *in vivo* assays of AmtB-LacZ and AmtB-PhoA fusions indicate that this protein has 12 transmembrane helices, with both the N-terminus and C-terminus in the cytoplasm [23]. There is also reason to suppose that Amt proteins may form oligomers in their native state. Experiments with transdominant mutants suggest that the *S. cerevisiae* Mep proteins can form heteromeric complexes *in vivo* [24] and the erythroid Rh proteins have been proposed to form a tetrameric complex [25].

We wish to develop *E. coli* AmtB as a model to address many of the questions relating to both the structure and function of this family of proteins. Here we report the hexahistidine tagging, overexpression and purification of the detergent-solubilized form of the protein. This has been used for experimental determination of quaternary structure by SDS/PAGE, gel-filtration chromatography, dynamic light scattering and sedimentation-equilibrium analytical ultracentrifugation.

MATERIALS AND METHODS

Strains and plasmids

The strains and plasmids used are listed in Table 1. For overexpression of the His-tagged protein encoded on pMM280 (AmtB6H) the coding sequence was cloned in two steps. Initially the 3′ 800 bp *Nde*I–*Bam*HI fragment was cloned into pT7-7. A PCR reaction to introduce a second *Nde*I site at the initiation codon was performed using the following oligonucleotide primers: AMT7 (GCTCTAGACATATGAAGATAGCGACGATA; with the *Nde*I site underlined) and AMT2 [35]. The product was *Nde*I-digested, ligated into the *Nde*I site of the initial pT7-7 construct and checked for the correct orientation and sequence; this plasmid was designated pMM285.

In vivo [^{14}C]methylamine transport assays

Assays were performed using the method described in [26], using modifications from [23]. [^{14}C]Methylamine hydrochloride (2.15 GBq/mmol) was obtained from Amersham Biosciences (Little Chalfont, Bucks., U.K.).

Transmission electron microscopy

Cells were grown as for *in vivo* methylamine transport assays. Samples of 500 μl were pre-fixed for 1 h in 2.5 % (v/v) glutaraldehyde by adding the appropriate amount of 25 % (v/v) glutaraldehyde directly to the cultures in an Eppendorf tube. The tubes were then spun briefly to pellet the bacteria into the base and, after removal of the culture medium, a small amount of 1 % (w/v) type VII low-gelling-temperature agarose (Sigma) in water at 37 °C was mixed with these cells. The tubes were then plunged into ice, the cells having been in agarose.

The samples were placed in tissue-handling devices and processed at low temperature to improve antigenicity as described by Wells [27] with the following modifications: infiltration steps were performed at −20 °C with LR White resin (Agar Scientific) plus 0.5 % (w/v) benzoin methyl ether, and polymerization was in Beem capsules (Agar Scientific), with indirect UV irradiation for 24 h at 20 °C followed by 16 h at room temperature. Sections were picked up on pyroxylin- and carbon-coated gold grids, stained with 2 % (w/v) uranyl acetate for 1 h and 1 % (w/v) lead citrate for 1 min, washed in water and air dried. The grids were viewed in a Jeol 1200 EX transmission electron microscope at 80 kV and photographs were taken on Kodak electron image film.

Protein quantification

Assays on whole-cell clarified lysates and subcellular fractions were performed with the Bio-Rad Protein Assay system using BSA as a standard. Purified AmtB6H concentration was measured spectroscopically at 280 nm (A_{280}) and computed using a molar absorption coefficient of 66890 $M^{-1} \cdot cm^{-1}$ [28].

Overexpression and purification of AmtB6H

C43 (pMM285) cells were grown aerobically overnight at 30 °C in nitrogen-limiting medium (M9 salts supplemented with 0.2 %

Table 1 Strains and plasmids

	Genotype or phenotype	Reference
Strain		
ET8000	*rbs lacZ*::IS*1 gyrA hutC*$_K$	[48]
GT1001	*rbs lacZ*::IS*1 gyrA hutC*$_K$ Δ*amtB*	[23]
BL21	F$^-$, *ompT, hsdS*$_B$, (r_B^-, m_B^-) *dcm, gal*, λ(DE3)	[49]
C41	BL21 derivative able to express membrane proteins	[36]
C43	C41 derivative with enhanced membrane-protein expression	[36]
Plasmid		
pACYC184	Medium-copy-number cloning vector	[50]
pGC1	*glnK amtB* in pACYC184	[35]
pGC2	*glnK amtB1* in pACYC184	[35]
pGC5	*glnK amtB2* in pACYC184	[35]
pGT11	*glnK amtB* in pWSK29	[35]
pMM280	*glnK amtB3* in pACYC184	[35]
pMM285	*amtB3* in pT7-7	The present study
pT7-7	T7 RNA polymerase-dependent expression vector	Details from M.M. on request
pWSK29	Low-copy-number cloning vector	[51]
pWVH141	*glnK amtB* in pBluescript-II SK$^+$	[7]

glucose, 200 μg/ml glutamine and 1 mM $MgSO_4$) plus 1 mM isopropyl β-D-thiogalactoside (IPTG) and 100 μg/ml carbenicillin. Cells were harvested by centrifugation at 2400 ***g*** at 4 °C for 10 min in an SLA-1500 rotor and resuspended in buffer 1 (50 mM Tris/HCl, pH 8.0/100 mM NaCl; 0.4 g of wet cells · ml^{-1}). Breakage was achieved by two passages through a French pressure cell at 110000 kPa at 4 °C. The extract was clarified by centrifugation for 30 min at 45000 ***g*** and 4 °C. The supernatant (whole-cell extract) was centrifuged at 210000 ***g*** for 1 h at 4 °C in Kendro Ultracrimp tubes in a TFT65-13 rotor using a Sorvall OTD-Combi ultracentrifuge. The membrane pellet was resuspended to 1.5 mg/ml protein in buffer 2 [50 mM Tris/HCl, pH 8.0/100 mM NaCl/10 % (v/v) glycerol] and frozen overnight at −70 °C, and the cytoplasmic supernatant was reserved for Western-blot analysis. The membranes were thawed on ice, and 10 % (w/v) dodecyl β-D-maltoside (DDM) in buffer 2 was added dropwise to a final concentration of 1 % (w/v) DDM. This was stirred at 4 °C for 2.5 h and the solubilized membranes were centrifuged at 210000 ***g*** for 1 h as before. The resultant supernatant (10 ml) was applied to a 1 ml Hi-Trap chelating column (Pharmacia Biotech) prepared by saturation with 100 mM $NiCl_2$, and equilibration with buffer 3 [50 mM Tris/HCl, pH 8.0/100 mM NaCl/10 % (v/v) glycerol/0.03 % DDM/10 mM imidazole] at 0.5 ml · min^{-1}. The protein-charged column was washed with 10 ml of buffer 3, and the protein eluted with a linear gradient of buffer 4 [50 mM Tris/HCl, pH 8.0/100 mM NaCl/10 % (v/v) glycerol/0.03 % DDM/500 mM imidazole].

For anion-exchange chromatography the AmtB6H peak eluate from the Ni^{2+} column was dialysed against ion-exchange (IE) start buffer [50 mM Tris/HCl, pH 8.0/50 mM NaCl/10 % (v/v) glycerol/0.03 % DDM] for 3 h at 4 °C and then loaded on to a 1 ml HiTrap Q Sepharose column pre-equilibrated in IE start buffer. The protein was eluted using a linear gradient of IE end buffer [50 mM Tris/HCl, pH 8.0/1 M NaCl/10 % (v/v) glycerol/0.03 % DDM]. For S12 gel-filtration chromatography, AmtB6H eluting from the Ni^{2+} column was concentrated by dialysis against buffer 5 [50 mM Tris/HCl, pH 8.0/250 mM NaCl/50 % (v/v) glycerol/0.03 % DDM]. A sample of 500 μl was loaded on to an S12 column pre-equilibrated with gel-filtration buffer [50 mM Tris/HCl, pH 8.0/250 mM NaCl/10 % (v/v) glycerol/0.03 % DDM] and run at 0.2 ml · min^{-1} using the same buffer. The S12 gel-filtration column was calibrated using 0.5 mg samples of the following in gel-filtration buffer: aprotinin, carbonic anhydrase, alcohol dehydrogenase, BSA, apoferritin, β-amylase and Dextran Blue (Sigma).

DDM binding to AmtB

The number of DDM molecules bound to purified AmtB6H in solution was determined using [^{14}C]DDM (2.03 GBq/mmol; a generous gift from Marc le Maire, Département de Biologie Cellulaire et Moléculaire, CEA, Centre d'Etudes de Saclay, Gif-sur-Yvette, France) as described previously by Friesen et al. [15]. The protein purified by anion-exchange chromatography was dialysed into IE start buffer. This was loaded on to a 1 ml HiTrap Q Sepharose column and washed with 30 ml of IE start buffer containing [^{14}C]DDM. The protein was eluted with a linear gradient of IE end buffer containing [^{14}C]DDM. The protein concentration of the peak was measured by the A_{280} and the DDM concentration calculated by liquid scintillation counting using a Wallac 1409 liquid scintillation counter.

Dynamic light scattering

Protein purified to the gel-filtration stage was diluted to 4.48 μM in gel-filtration buffer and analysed for dynamic light scattering in a DynaPro 99 (Protein Solutions) at 4, 20 and 37 °C. At each temperature 15 readings were recorded.

Analytical ultracentrifugation

Sedimentation-equilibrium experiments were performed in a Beckman Optima XL/I analytical ultracentrifuge using 12 mm-pathlength double-sector charcoal-filled Epon centrepieces in an AN-50Ti 8-place rotor at 20 °C. Protein samples were purified by S12 gel filtration and serially diluted to 2.24 and 4.48 μM protein in gel-filtration buffer. Sample volume was 110 μl. Experiments were conducted at 6700, 8000, 9500 and 12000 rev./min using the absorbance optics at 280 nm, to collect data at 0.001 cm intervals with 25 replicates. The data were analysed using the Beckman software supplied with the centrifuge.

Data were treated assuming a multi-component system [29]. The protein–detergent particles distribute in the centrifugal field according to eqn (1):

$$M(1-\varphi'\rho) = (2RT/\omega^2)\,\mathrm{d}(\ln c)/\mathrm{d}r^2 \quad (1)$$

where M is the molecular mass of the protein component in the particle, ρ is the solvent density, R is the gas constant, T is the temperature, ω is the angular velocity, c is the measured concentration and r is the radial position in the cell. The factor φ' is the partial specific volume of the protein–detergent complex. This may be broken down further according to eqn (2):

$$(1-\varphi'\rho) = (1-\bar{v}_{p'}\rho)+\delta_d(1-\bar{v}_{d'}\rho) \quad (2)$$

where $\bar{v}_{p'}$ is the partial specific volume of the protein, $\bar{v}_{d'}$ is that of the detergent and δ_d is the mass ratio, in g of detergent bound/g of protein, determined experimentally in this investigation. The partial specific volume of AmtB ($\bar{v}_{p'} = 0.7536\ cm^3/g$ at 20 °C) and the buffer density ($\rho = 1.03787\ g/cm^3$) were calculated using the program SEDNTERP [30].

A critical parameter in calculating the protein content of the complex following equilibrium sedimentation is the density, and therefore the partial specific volume ($\bar{v}_d$), of the detergent. Several measurements of density and $\bar{v}_d$ have been made for DDM and values range between 0.809 and 0.901 cm^3/g [31,32]. However, of the seven independent estimates, six were very similar, giving a mean estimate of $0.824 \pm 0.01\ cm^3/g$, whereas the seventh (0.901 cm^3/g) was significantly different. The latter estimate differs from the others in that it is for the hydrated value of the detergent [32] and we therefore used a value of 0.824 cm^3/g, which has previously given the correct mass for other proteins, such as CaATPase and FhuA [33,34].

SDS/PAGE and Western-blot analysis

Unless otherwise stated, samples for SDS/PAGE were not boiled prior to loading on to the gel. Pre-treatment with β-mercaptoethanol of Ni^{2+}-column affinity-purified protein was by addition of a water/β-mercaptoethanol mixture to give final concentrations of 0–25 % (v/v) β-mercaptoethanol in the sample, incubation on ice for 5 min, followed by addition of loading buffer before loading on the gel. For Western blots of whole-cell sonicates, cells were grown as for [^{14}C]methylamine transport assays, 5 ml were harvested by centrifugation and resuspended in 200 μl of buffer S1 (50 mM Tris/HCl, pH 8.0/100 mM EDTA), and lysed on ice by sonication at 10 μm amplitude, for five cycles of 10 s on/10 s off. For blots of subcellular fractions of C43 (pMM285), samples taken during purification were used. After transfer on to Hybond-ECL nitrocellulose membrane (Amersham Bioscience) the extracts were incubated with anti-tetrahistidine antibody (Qiagen) and detected using the ECL system

(Amersham Bioscience). Following detection, membranes were stained with Coomassie Brilliant Blue to confirm uniformity of transfer.

RESULTS

Hexahistidine tagging and overexpression of AmtB

To facilitate the purification of *E. coli* AmtB we chose to add a C-terminal hexahistidine tag. As AmtB proteins from a variety of bacteria show considerable conservation right up to the C-terminus (e.g. Tyr-426 is a highly conserved residue), we separated the histidine tag from the native C-terminus by a linker sequence of 10 residues (DQAQQPAQAD) with the intention that this might improve accessibility of the histidine tag in the native protein and thereby increase the efficiency of the Ni^{2+}-affinity chromatography. The accessibility of the histidine tag was compared with a construct in which no linker sequence was present between the tag and the native C-terminus by Western blotting whole-cell extracts from strains expressing each variant using an anti-tetrahistidine antibody. The construct with the linker showed a significantly stronger reaction, suggesting that accessibility was improved by the linker (results not shown).

Three derivatives of the wild-type *amtB* gene were constructed: *amtB1*, which has two extra C-terminal residues; *amtB2*, which encodes the C-terminal 10-residue linker; and *amtB3*, which encodes a hexahistidine tag after the linker [35]. In all these constructs, carried in pGC2, pGC5 and pMM280, respectively, *amtB* is expressed from the native p*glnK* promoter and is consequently inducible by nitrogen limitation (Figure 1). The *in vivo* activity of the modified AmtB proteins was assessed by [^{14}C]methylamine transport assays using strain GT1001 (Δ*amtB*) carrying each of the plasmids, pGC2, pGC5 and pMM280, and in each case the modified forms of AmtB showed transport activities comparable with the wild-type, encoded by pGC1 (Table 2).

For overexpression of *amtB3* the coding sequence from pMM280 was cloned into pT7-7 to give pMM285. The usual host for such constructs is *E. coli* BL21, in which high-level expression of the cloned gene from a T7 RNA polymerase-dependent promoter is inducible by IPTG. However, as overexpression of membrane proteins can often be lethal, we also used two mutant derivatives of BL21 (C41 and C43) that have been demonstrated to facilitate high-level expression of a number of membrane proteins [36]. To test for overexpression *in vivo*, we determined the rates of [^{14}C]methylamine transport in strains BL21, C41 and C43, all carrying pMM285. In the presence of inducer, growth of BL21 and C41 was considerably impaired when they carried pMM285, whereas strain C43 (pMM285) grew normally (results not shown). The only significant elevation of activity above that expected from a chromosomally encoded AmtB was in C43 (pMM285), which had 40-fold greater activity than C43 alone (Table 2).

Table 2 *In vivo* [^{14}C]methylamine transport assays

Rates were linear over the entire assay.

Strain	Relevant genotype	Transport activity (nmol of [^{14}C]methylamine/ mg of biomass per min)
E. coli K12		
GT1001	Δ*amtB*	0.1 ± 0.05
GT1001 (pGC1)	Δ*amtB* (*amtB*$^+$)	6.74 ± 1.8
GT1001 (pGC2)	Δ*amtB* (*amtB1*)	6.96 ± 0.91
GT1001 (pGC5)	Δ*amtB* (*amtB2*)	4.7 ± 0.72
GT1001 (pMM280)	Δ*amtB* (*amtB3*)	6.14 ± 2.02
E. coli B		
BL21	*amtB*$^+$	4.01 ± 0.51
C41	*amtB*$^+$	4.16 ± 1.07
C43	*amtB*$^+$	4.76 ± 1.45
BL21 (pMM285)	*amtB*$^+$ (*amtB3*)	4.5 ± 1.62
C41 (pMM285)	*amtB*$^+$ (*amtB3*)	4.35 ± 4.02
C43 (pMM285)	*amtB*$^+$ (*amtB3*)	189.98 ± 65.0

Detection and localization of overexpressed AmtB

Having achieved a considerable increase in AmtB activity we wished to examine the localization of the overproduced protein and its behaviour on SDS/PAGE. Western-blot analysis of subcellular fractions of C43 (pMM285) showed that AmtB6H is contained solely within the membrane rather than in the cytoplasmic fraction (Figure 2, lanes 2–4). Similar results were obtained when *amtB* was expressed from its natural promoter, i.e.

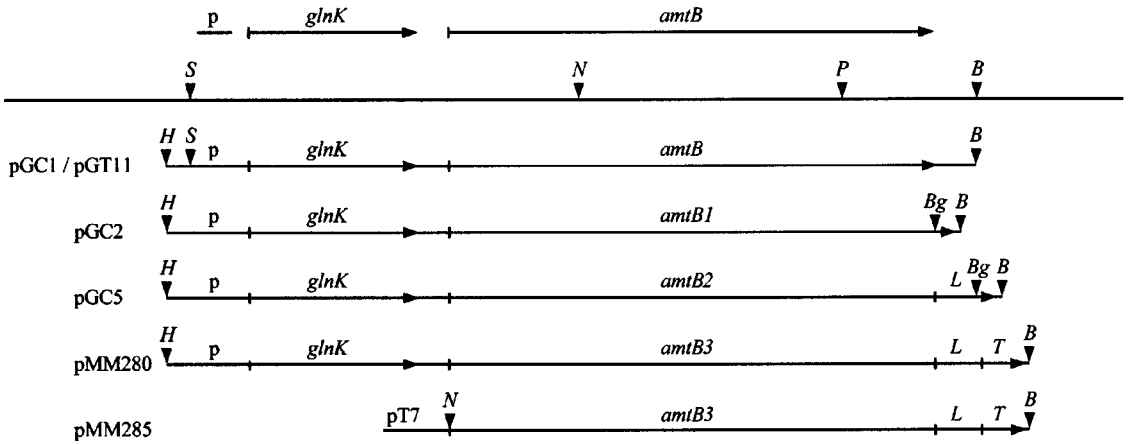

Figure 1 Map of *amtB* plasmids

Restriction sites shown are: B, *Bam*HI; Bg, *Bgl*II; H, *Hin*dIII; N, *Nde*I; P, *Pvu*I; S, *Sal*I. *L* marks the C-terminal linker region, *T* the hexahistidine tag and p indicates the promoter of the *glnKamtB* operon.

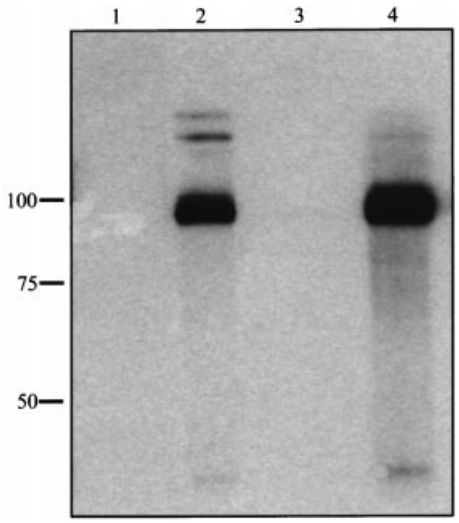

Figure 2 Over-produced AmtB6H is directed to the membrane

Western blot of protein extracts (3.5 μg of protein/lane) from cells grown under conditions of nitrogen limitation, probed with anti-tetrahistidine antibody. Lane 1 (control), clarified sonicate of strain GT1001 (pGC5). Lanes 2–4, C43 (pMM285) grown with 1 mM IPTG to induce the expression of AmtB6H: lane 2, whole-cell clarified lysate; lane 3, 210000 ***g*** supernatant (cytoplasm); lane 4, 210000 ***g*** pellet (membrane). Relative positions of molecular-mass markers (kDa) are shown at the left-hand side.

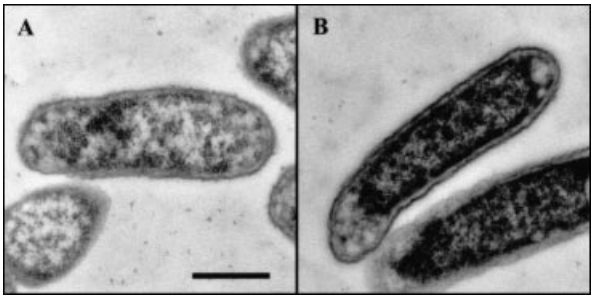

Figure 3 Over-produced AmtB6H induces no internal membrane proliferation

Electron micrographs of thin sections of *E. coli* cells grown overnight under conditions of nitrogen limitation with 1 mM IPTG to induce the expression of AmtB6H. (**A**) C43 (pMM285) overproducing AmtB6H; (**B**) control C43 cells. Scale bar, 0.5 μm.

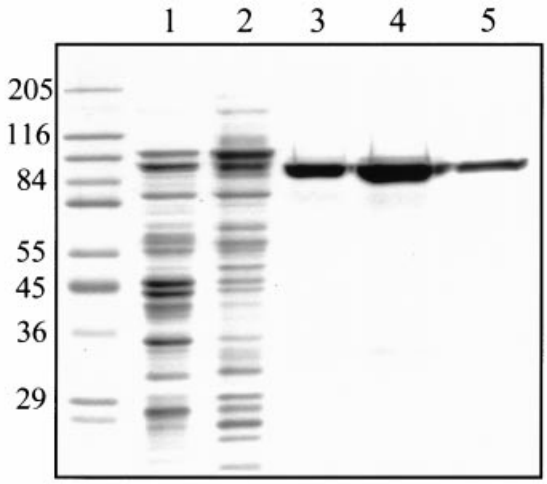

Figure 4 Purification of AmtB6H

SDS/PAGE (10% gel) stained with Coomassie Brilliant Blue, showing purification of AmtB6H from C43 (pMM285) cells. Lane 1, clarified cell lysate (15 μg of protein); lane 2, membrane extract (15 μg of protein); lane 3, peak fraction of Ni^{2+}-affinity chromatography (4 μg of protein); lane 4, peak fraction of anion-exchange chromatography (5 μg of protein); lane 5, peak fraction of size-exclusion chromatography (3 μg of protein). Molecular-mass markers (kDa) are shown on the left.

in GT1001 (pMM280) (results not shown). Previous studies have shown that over-production of subunit b of *E. coli* F_1F_o-ATP synthase in C43 is accompanied by marked proliferation of intracellular membranes that contain all the overexpressed protein [37]. However, electron micrographs of thin sections of C43 (pMM285) before and after induction showed no evidence of membrane proliferation (Figure 3).

In extracts prepared from both C43 (pMM285) and GT1001 (pMM280), the major AmtB band on SDS/PAGE ran at $\approx$ 90 kDa with minor species at around 33, 120 and 150 kDa (Figure 2). The estimated monomeric mass of AmtB from primary sequence is 44.5 kDa; however, membrane proteins often run with an aberrantly low apparent molecular mass on SDS/PAGE [38] and we assume that the lowest (33 kDa) band is the monomeric species. The fact that the majority of the protein runs at a significantly higher molecular mass suggests that this could be an oligomeric species.

AmtB purification and assessment of particle size

AmtB6H was extracted with 1% (w/v) DDM from the membrane fraction of C43 (pMM285) cells grown overnight in nitrogen-limiting conditions. The protein was isolated to at least 95% purity by Ni^{2+}-affinity chromatography (Figure 4, lanes 1–3), which could be improved to > 98% purity by either anion-exchange chromatography or size-exclusion gel filtration (Figure 4, lanes 4 and 5 respectively). In gel-filtration chromatography the protein eluted as a single symmetrical peak, indicating behaviour as a homogeneous species (results not shown). From the UV absorption of the Ni^{2+}-affinity-purified protein samples it was estimated that the yield was $\approx$ 1 mg/l of cells.

The purified protein species ran at $\approx$ 90 kDa on SDS/PAGE, correlating with the size of the major species identified in cell extracts by Western blotting. These observations, while suggestive of a native oligomer, do not provide direct information on the actual molecular mass of the protein owing to the recognized aberrant behaviour of membrane proteins on SDS/PAGE and the fact that the detergent-solubilized protein is actually a complex, in which each molecule of protein is bound to an unknown number of detergent molecules.

The purified material was used to obtain two independent estimates of the size of the protein–detergent complex. The Stokes radius (R_S) of the complex can be estimated from size-exclusion chromatography. Calibration of a Superose 12 column with globular proteins of known R_S values was performed and from the curve of R_S against $(V_e - V_o)/(V_t - V_o)$, where V_e represents the elution volume, V_o the void volume and V_t the total column volume, the R_S of the complex was estimated to be 5.25 nm. The same data were used to calculate the predicted molecular mass of the complex using the plot of log molecular mass against V_e/V_o, giving a value of 235 kDa.

Dynamic light scattering of gel-filtration-purified AmtB6H was performed to assay for aggregation of the protein, and as a

Table 3 Dynamic light scattering

Temperature (°C)	Hydrodynamic radius (nm)	Polydispersity (%)	Mass estimate (kDa)
4	6.52	24.3	273
20	5.53	20.3	183
37	5.72	20.3	199

second estimate of the protein–detergent particle size. The purified protein showed no indication of aggregation at 4, 20 or 37 °C, having a polydispersity figure of $\approx 20\,\%$ (Table 3), and the particle size (5.5–6.5 nm) correlated well with the estimate obtained by size-exclusion chromatography.

DDM binding to AmtB

The most rigorous estimate of the molecular mass of the detergent–protein complex can be obtained by analytical centrifugation, but such an analysis requires an independent estimate of the molar ratio of DDM/AmtB in the complex. This ratio was therefore first measured using equilibrium column desorption [15,39]. AmtB6H was bound to a Q Sepharose column and equilibrated with buffer containing [^{14}C]DDM. The concentration of labelled DDM eluting from the column in this wash step was monitored by liquid scintillation counting. The counts plateaued between 7.5 and 20 ml (results not shown) and therefore equilibration was terminated after washing with 30 ml of labelled buffer.

Elution of the protein with a linear gradient of NaCl produced a rise in DDM concentration that matched the profile of the protein peak (Figure 5A). The relationship between the increase in [^{14}C]DDM concentration and AmtB6H concentration was linear from 1.5 to 9.0 μM protein, and linear-regression analysis of the combined data from two independent experiments gave a value of 88.6 ± 2.8 DDM molecules bound to each AmtB6H molecule (Figure 5B). This corresponds to a mass contribution of 45.3 ± 1.4 kDa and therefore the mass ratio (δ_d) DDM/AmtB is 1.03 ± 0.03.

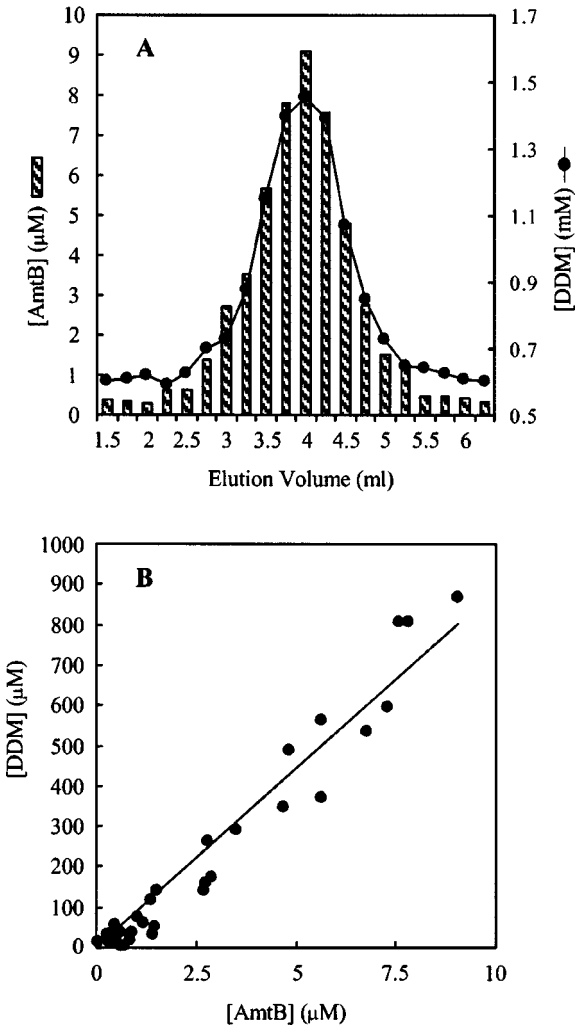

Figure 5 (A) DDM binding to AmtB6H and (B) linear regression to calculate DDM/AmtB6H ratio

(**A**) Concentrations of AmtB6H (hatched bars) and DDM (●), eluting from a 1 ml HiTrap-Q Sepharose column. Only one data set is shown. (**B**) The DDM concentration associated with the protein peak is plotted against protein concentration; combined data from two experiments are shown with the line of best fit determined by linear regression.

Analytical ultracentrifugation

To determine the hydrodynamic properties of DDM-solubilized AmtB we employed sedimentation-equilibrium analytical centrifugation. Experiments were conducted at two protein concentrations, 2.24 and 4.48 μM, and data were acquired after attainment of equilibrium at speeds of 6700, 8000, 9500 and 12000 rev./min. Plots of the natural log of the absorbance versus the square of the radial position in the ultracentrifuge cell were linear at both concentrations and all speeds, implying that no aggregation or change in oligomeric state occurs with changes of concentration. Plots of the apparent molecular mass as a function of concentration gave constant and consistent values across both concentrations and all four speeds. Furthermore, simultaneous analysis of data from both concentrations and all four speeds produced the same apparent molecular mass (within the limits of experimental error) as for the individual speeds. This indicates that the AmtB6H–DDM complex behaves as a single species with neither aggregation to larger oligomers nor dissociation to smaller species over the accessible concentration range.

The data were then fitted by non-linear least-squares analysis to a single species model (Figure 6A) and examination of the residuals did not justify inclusion of extra terms for association or non-ideality (Figure 6B). The value obtained for $M(1-\varphi'\rho)$ was 46690 ± 450 Da. Using eqn (2) (see the Materials and methods section) with $\delta_d = 1.03 \pm 0.03$, as determined using radioactive DDM, and $\bar{v}_d = 0.824$ yields a molecular mass of 127 ± 17 kDa, which implies that the protein in the particles is present as a trimer (predicted as 133.5 kDa).

Effects of reduction and boiling

The behaviour of the detergent-solubilized protein as a trimer in analytical ultracentrifugation was consistent with the failure of the protein to behave as a monomer on SDS/PAGE, both in Western-blot analysis of whole-cell extracts and after purification. This suggested that the complex was highly resistant to dissociation by SDS and we therefore investigated its stability further by examining the effects of reduction or boiling of the protein prior to SDS/PAGE. Pre-treatment of AmtB with increasing concentrations of β-mercaptoethanol (up to a maximum of 25 %, v/v) prior to addition of sample buffer led to a progressive increase in the formation of a ≈ 33 kDa species, and

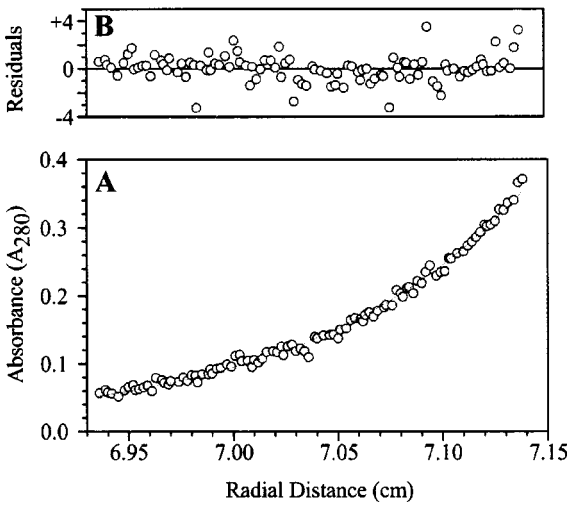

Figure 6 Analytical ultracentrifugation sedimentation-equilibrium data

(**A**) The equilibrium profile of AmtB6H at 8000 rev./min with a starting concentration of 2.24 μM. (**B**) The residuals of the line of best fit.

at concentrations of $\geqslant 15\,\%$ (v/v) species at ≈ 66 and ≈ 95 kDa were also apparent (Figure 7A).

The combined effects of boiling under reducing and non-reducing conditions were also tested. Protein samples were prepared in Laemmli sample buffer with or without 5 % (v/v) β-mercaptoethanol and then either immediately loaded on to an SDS/PAGE (10 %) gel or boiled for 1 or 5 min before loading. Unboiled samples in both reducing and non-reducing conditions showed a major band at ≈ 90 kDa and a minor species at 33 kDa (Figure 7B, lanes 1 and 2 respectively). Boiling for 1 min completely destroyed the 90 kDa band, and lead to the formation of a ladder of species from ≈ 33 kDa, increasing in 30 kDa steps, although non-reducing conditions produced fewer higher-order species than reducing conditions (Figure 7B, lanes 3 and 4). Boiling for 5 min under reducing conditions created a single aggregated species that just entered the resolving gel (Figure 7B, lane 5), whereas under non-reducing conditions the ladder of species remained (Figure 7B, lane 6).

DISCUSSION

The *E. coli* ammonium-transport protein AmtB provides a model system for analysis of the structure and function of proteins in the Amt family, which are found in bacteria, fungi, plants and animals and have been shown recently to include the human Rh proteins. The purification of AmtB is a prerequisite for many experiments addressing both the structure and function of this novel family of membrane proteins and we have therefore engineered the *E. coli amtB* gene to facilitate overexpression and purification of the protein.

Topological analysis of AmtB indicates that the C-terminal 32 amino acids constitute a cytoplasmically located domain of the protein within which a number of residues are highly conserved. This C-terminal domain can be considerably longer in other Amt proteins, being some 90–100 residues in the *S. cerevisiae* Mep proteins and between 130 and 180 residues in *C. elegans* Amt proteins. Deletion of this region from the *E. coli* AmtB protein does not abolish activity [35]. We found that the addition of a hexahistidine tag, joined to the C-terminus by a 10-amino acid linker, did not impair the [^{14}C]methylamine transport activity of the protein and we conclude that the histidine tag does not significantly affect the functional conformation of the protein.

Overexpression of AmtB in *E. coli* BL21 was highly deleterious to growth, a situation that is quite commonly observed for integral membrane proteins. This problem was overcome for a number of membrane proteins by the direct selection of two spontaneous mutants of BL21, C41 and C43, with improved growth characteristics [36]. The mutations carried by these two derivative strains are uncharacterized (B. Miroux and J. Walker, personal communication). The growth impairment caused by overexpression of AmtB was essentially completely overcome in C43, and we observed a concomitant 40-fold increase in [^{14}C] methylamine transport. Overexpression of subunit b of *E. coli* F_1F_o-ATP synthase in C43 has been shown to result in proliferation of intracellular membranes that contain all the overexpressed protein [37], but this was not observed for overproduction of AmtB in C43. Indeed, fragments of F_1F_o-ATP synthase have been overproduced in C43 without internalized membranes, and the link between membrane proliferation and successful overexpression is not clear [37].

Purification of the AmtB6H protein by Ni^{2+}-affinity chromatography was extremely effective, giving an excellent yield with very few contaminating proteins, such that after ion-exchange chroma-

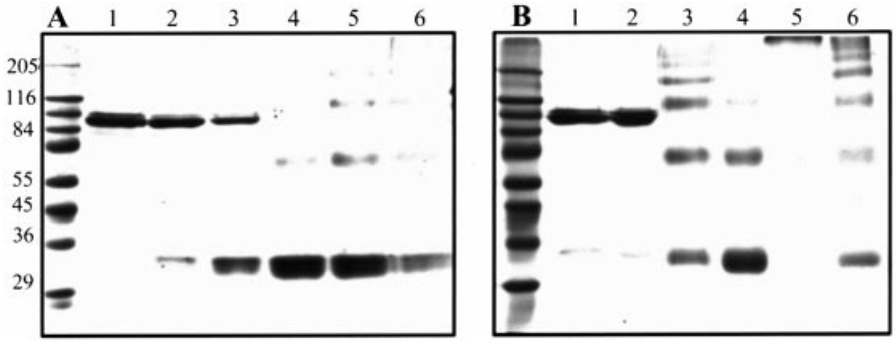

Figure 7 (A) Effect of β-mercaptoethanol treatment on AmtB prior to loading and (B) effects of combined boiling and β-mercaptoethanol on AmtB

(**A**) SDS/PAGE (10% gel) of Ni^{2+}-affinity-purified AmtB6H preincubated for 5 min at 0 °C with β-mercaptoethanol (5 μg of protein/lane). Lanes 1–6, pre-treatment with 0, 5, 10, 15, 20 and 25% (v/v) β-mercaptoethanol respectively. (**B**) SDS/PAGE (10% gel) of Ni^{2+}-affinity-purified AmtB6H (5 μg of protein). Lanes 1 and 2, not boiled; lanes 3 and 4, boiled for 1 min; lanes 5 and 6, boiled for 5 min. Lanes 1, 3 and 5, with β-mercaptoethanol; lanes 2, 4 and 6, without β-mercaptoethanol.

tography the protein was judged to be > 98 % pure. The protein is stable in the purified state and during analytical ultracentrifugation the protein was maintained at 20 °C for 90 h with no indication of degradation. On SDS/PAGE AmtB did not migrate with the predicted monomeric mass of 44.5 kDa, and a species running at ≈ 33 kDa was likely to be the monomeric form. Such aberrant mobility on SDS/PAGE is a common feature of membrane proteins and it is notable that the RhD and RhCE polypeptides, which are related to AmtB, are designated Rh30 because although their predicted molecular mass is 45.5 kDa, their apparent molecular mass on SDS/PAGE is around 30 kDa [40]. However, the dominant form of AmtB in whole-cell extracts has an apparent molecular mass of ≈ 90 kDa, suggesting that in its native state the protein is oligomeric. The purified protein has the same apparent molecular mass on SDS/PAGE, suggesting that the native quaternary structure is not dissociated by SDS.

Such resistance to dissociation by SDS has also been seen with other membrane proteins, e.g. the tetrameric AqpZ aquaporin from *E. coli* [41], the prokaryotic K^+ channel [42] and the calcium regulatory protein phospholamban [43]. Treatment of purified AmtB by boiling and/or reducing agents produces a ladder of species that increase in size by apparent increments of ≈ 30 kDa, and we interpret these bands to reflect increasing multimers of the protein formed by aggregation. Similar treatments were also effective in dissociating AqpZ and phospholamban oligomers, and in each case mutations of specific cysteine residues in the protein diminished the oligomer's stability [41,43]. However, in both cases the involvement of disulphide bonds was excluded and it would appear that hydrophobic interactions among the transmembrane helices are the predominant forces in stabilizing the oligomer [43]. *E. coli* AmtB contains eight cysteine residues, all but one of which are predicted to be located within transmembrane helices and none of which are conserved residues in Amt proteins [23]. Furthermore, just as with phospholamban [44], dissociation can be achieved by boiling briefly in SDS without a reducing agent and we consider that this suggests strongly that the trimer is not stabilized by intersubunit disulphide bonds.

Hydrodynamic characterization of the DDM-solubilized AmtB shows the protein to behave as a single thermodynamic species which purifies as a stable trimer. This result is consistent with the behaviour of the protein on SDS/PAGE, both in whole-cell extracts and after purification. The concept that the functional form of AmtB in the cell membrane is trimeric is also supported by our recent studies on the interaction between AmtB and the signal-transduction protein GlnK. In bacteria and archaea the *amtB* gene is invariably linked to *glnK*, which encodes a member of the P_{II} signal-transduction family, which are proteins that regulate enzyme activity and gene expression in response to intracellular nitrogen status. We suggested previously that this conserved linkage may reflect a physical interaction between the two proteins [45] and we have now shown that in *E. coli* GlnK binds to the membrane in an AmtB-dependent manner and that GlnK acts as a negative regulator of the transport activity of AmtB [35]. The P_{II} proteins, including GlnK, are trimers but to date the reason for this quaternary structure has not been apparent, particularly as none of their known targets have trigonal symmetry. However, we now consider it likely that GlnK and AmtB evolved in concert and the trimeric structure of both proteins reflects a symmetry required for optimal interaction between the two proteins.

Independent experimental data suggest that the native state of other members of the Amt family is also multimeric. *S. cerevisiae* synthesizes three ammonium-transport proteins, Mep1, Mep2 and Mep3. The 26972c strain of *S. cerevisiae*, used originally for cloning ammonium-transporter genes, contains two mutations (*mep1-1* and *mep2-1*) and cannot grow on low concentrations (1 mM) of ammonium, whereas cells with a complete deletion of each of the genes (*mep1*Δ, *mep2*Δ) grow normally owing to the presence of the third transporter encoded by *mep3* [46]. Genetic analysis has shown that the phenotype of strain 26972c is caused by the *trans*-inhibition of Mep3 by an inactive form of Mep1 encoded by *mep1-1*. The *mep1-1* gene encodes a form of Mep1 with a Gly-413 → Asp substitution. This glycine residue is highly conserved in Amt proteins (Gly-415 in *E. coli* AmtB) and lies within the C-terminal cytoplasmic domain. The growth inhibition caused by *mep1-1* can also be overcome by expressing *mep3* on a high-copy-number plasmid and increasing the Mep3 protein dosage. These observations indicate that the *S. cerevisiae* Mep proteins may form a complex in the membrane, although this putative association into heteromeric complexes is not essential for ammonium transport as the Mep proteins are individually active when expressed alone in a triple *mep*-deletion strain. Furthermore, immunoblots for all three Mep proteins show signals compatible with the existence of homomultimers [21].

The human Rh proteins, now also known to be ammonium transporters and members of the Amt family, have been proposed to associate in a multimolecular complex in the erythrocyte membrane. The size of the Rh complex was analysed by ultracentrifugation and, after correction for the amount of detergent (Triton X-100) bound to the complex, the apparent molecular mass was estimated as 170 kDa [47]. Taken together with other studies on the organization of the complex, this led to a model based on an $\alpha_2\beta_2$ tetramer made up of two RhAG molecules and two RhCE or RhD molecules [25]. However, it should be noted that, in discussing their estimation of the molecular mass of the complex, Hartel-Schenk and Agre [47] acknowledge that the value of 170 kDa "reflects the imprecisions inherent in determining the physical size of a hydrophobic membrane protein" and there is presently no independent evidence for the stoichiometry of RhAG/RhD or RhAG/RhCE being 1 : 1. As with the yeast Mep proteins, the heteromeric nature of the complex is also apparently not a prerequisite for ammonium-transport activity, because RhAG expressed alone in the *S. cerevisiae* triple *mep*-deletion strain has transport activity [5].

In conclusion there is evidence to suggest that the primary and secondary structures of a number of members of the Amt protein family are similar and that different members of the family can functionally substitute for each other. It is therefore tempting to consider the possibility that higher-order structure in these proteins is also conserved. The purification of AmtB now offers the possibility of exploring more detailed functional and structural studies that could be relevant to the whole protein family.

We thank Claire Stevenson for help with dynamic-light-scattering analysis and Marc le Maire (Département de Biologie Cellulaire et Moléculaire, CEA, Centre d'Etudes de Saclay, Gif-sur-Yvette, France) for the gift of [^{14}C]DDM and advice on its use. D.B., K.F. and M.M. were supported by a grant in aid from the Biotechnology and Biological Sciences Research Council (BBSRC) to the John Innes Centre. G.H.T. was supported by a grant from the Commission of the European Communities (EURATINE: BIOTECH94-2310). G.C. acknowledges a BBSRC studentship.

REFERENCES

1 van Dommelen, A., de Mot, R. and Vanderleyden, J. (2001) Ammonium transport: unifying concepts and unique aspects. Aust. J. Plant Physiol. **28**, 959–967

2 Marini, A.-M., Vissers, S., Urrestarazu, A. and Andre, B. (1994) Cloning and expression of the MEP1 gene encoding an ammonium transporter in *Saccharomyces cerevisiae*. EMBO J. **13**, 3456–3463

3 Ninnemann, O., Jauniaux, J.-C. and Frommer, W. B. (1994) Identification of a high affinity NH_4^+ transporter from plants. EMBO J. **13**, 3464–3471

4 Marini, A.-M., Urrestarazu, A., Beauwens, R. and Andre, B. (1997) The Rh (rhesus) blood group polypeptides are related to NH_4^+ transporters. Trends Biochem. Sci. **22**, 460–461

5 Marini, A.-M., Matassi, G., Raynal, V., Andre, B., Cartron, J. P. and Cherif-Zahar, B. (2000) The human Rhesus-associated RhAG protein and a kidney homologue promote ammonium transport in yeast. Nat. Genet. **26**, 341–344

6 Liu, Z., Peng, J., Mo, R., Hui, C. and Huang, C. H. (2001) Rh type B glycoprotein is a new member of the Rh superfamily and a putative ammonia transporter in mammals. J. Biol. Chem. **276**, 1424–1433

7 van Heeswijk, W. C., Hoving, S., Molenaar, D., Stegeman, B., Kahn, D. and Westerhoff, H. V. (1996) An alternative P_{II} protein in the regulation of glutamine synthetase in *Escherichia coli*. Mol. Microbiol. **21**, 133–146

8 Kleiner, D. (1985) Bacterial ammonium transport. FEMS Microbiol. Rev. **32**, 87–100

9 Meier-Wagner, J., Nolden, L., Jakoby, M., Siewe, R., Krämer, R. and Burkovski, A. (2001) Multiplicity of ammonium uptake systems in *Corynebacterium glutamicum*: role of Amt and AmtB. Microbiology **147**, 135–143

10 Siewe, R. M., Weil, B., Burkovski, A., Eikmanns, B. J., Eikmanns, M. and Krämer, R. (1996) Functional and genetic characterisation of the (methyl)ammonium uptake carrier of *Corynebacterium glutamicum*. J. Biol. Chem. **271**, 5398–5403

11 Ludewig, U., von Wirén, N. and Frommer, W. B. (2002) Uniport of NH_4^+ by the root hair plasma membrane ammonium transporter LeAMT1;1. J. Biol. Chem. **277**, 13548–13555

12 Howitt, S. and Udvardi, M. (2000) Structure, function and regulation of ammonium transporters in plants. Biochem. Biophys. Acta **1465**, 152–170

13 Montesinos, M. L., Muro-Pastor, A. M., Herrero, A. and Flores, E. (1998) Ammonium/methylammonium permeases of a cyanobacterium. Identification and analysis of three nitrogen-regulated *amt* genes in *Synechocystis* sp. PCC 6803. J. Biol. Chem. **273**, 31463–31470

14 Soupene, E., He, L., Yan, D. and Kustu, S. (1998) Ammonia acquisition in enteric bacteria: physiological role of the ammonium/methylammonium transport B (AmtB) protein. Proc. Natl. Acad. Sci. U.S.A. **95**, 7030–7034

15 Friesen, R. H., Knol, J. and Poolman, B. (2000) Quaternary structure of the lactose transport protein of *Streptococcus thermophilus* in the detergent-solubilized and membrane-reconstituted state. J. Biol. Chem. **275**, 33527–33535

16 Zhuang, J., Privé, G. G., Werner, G. E., Ringler, P., Kaback, H. R. and Engel, A. (1999) Two-dimensional crystallization of *Escherichia coli* lactose permease. J. Struct. Biol. **125**, 63–75

17 Yin, C. C., Aldema-Ramos, M. L., Borges-Walmsley, M. I., Taylor, R. W., Walmsley, A. R., Levy, S. B. and Bullough, P. A. (2000) The quarternary molecular architecture of TetA, a secondary tetracycline transporter from *Escherichia coli*. Mol. Microbiol. **38**, 482–492

18 Wang, D. N., Sarabia, V. E., Reithmeier, R. A. F. and Kühlbrandt, W. (1994) Three-dimensional map of the dimeric membrane domain of human erythrocyte anion exchanger, band 3. EMBO J. **13**, 3230–3235

19 Williams, K. A. (2000) Three-dimensional structure of the ion-coupled transport protein NhaA. Nature (London) **403**, 112–115

20 Tate, C. G., Kunji, E. R. S., Lebendiker, M. and Schuldiner, S. (2001) The projection structure of EmrE, a proton-linked multidrug transporter from *Escherichia coli*, at 7 Å resolution. EMBO J. **20**, 77–81

21 Marini, A.-M. and Andre, B. (2000) *In vivo N*-glycosylation of the Mep2 high-affinity ammonium transporter of *Saccharomyces cerevisiae* reveals an extracytosolic N-terminus. Mol. Microbiol. **38**, 552–564

22 Taté, R., Riccio, A., Merrick, M. and Patriarca, E. J. (1998) The *Rhizobium etli amtB* gene coding for an NH_4^+ transporter is down-regulated early during bacteroid differentiation. Mol. Plant–Microbe Interact. **11**, 188–198

23 Thomas, G. H., Mullins, J. G. and Merrick, M. (2000) Membrane topology of the Mep/Amt family of ammonium transporters. Mol. Microbiol. **37**, 331–344

24 Marini, A. M., Springael, J. Y., Frommer, W. B. and Andre, B. (2000) Cross-talk between ammonium transporters in yeast and interference by the soybean SAT1 protein. Mol. Microbiol. **35**, 378–385

25 Eyers, S. A., Ridgwell, K., Mawby, W. J. and Tanner, M. J. (1994) Topology and organization of human Rh (rhesus) blood group-related polypeptides. J. Biol. Chem. **269**, 6417–6423

26 Jack, R., De Zamaroczy, M. and Merrick, M. (1999) The signal transduction protein GlnK is required for NifL-dependent nitrogen control of *nif* gene expression in *Klebsiella pneumoniae*. J. Bacteriol. **181**, 1156–1162

27 Wells, B. (1985) Low temperature box and tissue handling device for embedding biological tissue for immunostaining in electron microscopy. Micron Microscop. Acta **16**, 49–53

28 Pace, C. N., Vajdos, F., Fee, L., Grimsley, G. and Gray, T. (1995) How to measure and predict the molar absorption coefficient of a protein. Protein Sci. **4**, 2411–2423

29 Clarke, S. (1975) The size and detergent binding of membrane proteins. J. Biol. Chem. **250**, 5459–5469

30 Laue, T. M., Shah, B. D., Ridgeway, T. M. and Pelletier, S. L. (1992) Computer-aided interpretation of analytical sedimentation data for proteins. In Analytical Ultracentrifugation in Biochemistry and Polymer Science (Harding, S. E., Rowe, A. J. and Horton, J. C., eds.), pp. 90–125, Royal Society of Chemistry, Cambridge

31 le Maire, M., Champeil, P. and Moller, J. V. (2000) Interaction of membrane proteins and lipids with solubilizing detergents. Biochim. Biophys. Acta **1508**, 86–111

32 Lustig, A., Engel, A., Tsiotis, G., Landau, E. M. and Baschong, W. (2000) Molecular weight determination of membrane proteins by sedimentation equilibrium at the sucrose or nycodenz-adjusted density of the hydrated detergent micelle. Biochim. Biophys. Acta **1464**, 199–206

33 Boulanger, P., le Maire, M., Bonhivers, M., Dubois, S., Desmadril, M. and Letellier, L. (1996) Purification and structural and functional characterization of FhuA, a transporter of the *Escherichia coli* outer membrane. Biochemistry **35**, 14216–14224

34 Champeil, P., Menguy, T., Tribet, C., Popot, J. L. and le Maire, M. (2000) Interaction of amphipols with sarcoplasmic reticulum Ca^{2+}-ATPase. J. Biol. Chem. **275**, 18623–18637

35 Coutts, G., Thomas, G., Blakey, D. and Merrick, M. (2002) Membrane sequestration of the signal transduction protein GlnK by the ammonium transporter AmtB. EMBO J. **21**, 1–10

36 Miroux, B. and Walker, J. E. (1996) Over-production of proteins in *Escherichia coli*: mutant hosts that allow synthesis of some membrane proteins and globular proteins at high levels. J. Mol. Biol. **260**, 289–298

37 Arechaga, I., Miroux, B., Karrasch, S., Huijbregts, R., de Kruijff, B., Runswick, M. J. and Walker, J. E. (2000) Characterisation of new intracellular membranes in *Escherichia coli* accompanying large scale over-production of the β subunit of F_1F_0 ATP synthase. FEBS Lett. **482**, 215–219

38 Gaillard, I., Slotboom, D. J., Knol, J., Lolkema, J. S. and Konings, W. N. (1996) Purification and reconstitution of the glutamate carrier GltT of the thermophilic bacterium *Bacillus stearothermophilus*. Biochemistry **35**, 6150–6156

39 Moller, J. V. and le Maire, M. (1993) Detergent binding as a measure of hydrophobic surface area of integral membrane proteins. J. Biol. Chem. **268**, 18659–18672

40 Avent, N. D., Ridgwell, K., Tanner, M. J. and Anstee, D. J. (1990) cDNA cloning of a 30 kDa erythrocyte membrane protein associated with Rh (Rhesus)-blood-group-antigen expression. Biochem. J. **271**, 821–825

41 Borgnia, M. J., Kozono, D., Calamita, G., Maloney, P. C. and Agre, P. (1999) Functional reconstitution and characterization of AqpZ, the *E. coli* water channel protein. J. Mol. Biol. **291**, 1169–1179

42 Heginbotham, L., Odessey, E. and Miller, C. (1997) Tetrameric stoichiometry of a prokaryotic K^+ channel. Biochemistry **36**, 10335–10342

43 Fujii, J., Maruyama, K., Tada, M. and MacLennan, D. H. (1989) Expression and site-specific mutagenesis of phospholamban. Studies of residues involved in phosphorylation and pentamer formation. J. Biol. Chem. **264**, 12950–12955

44 Simmerman, H. K., Collins, J. H., Theibert, J. L., Wegener, A. D. and Jones, L. R. (1986) Sequence analysis of phospholamban. Identification of phosphorylation sites and two major structural domains. J. Biol. Chem. **261**, 13333–13341

45 Thomas, G., Coutts, G. and Merrick, M. (2000) The *glnKamtB* operon: a conserved gene pair in prokaryotes. Trends Genet. **16**, 11–14

46 Marini, A.-M., Soussi-Boudekou, S., Vissers, S. and Andre, B. (1997) A family of ammonium transporters in *Saccharomyces cerevisae*. Mol. Cell. Biol. **17**, 4282–4293

47 Hartel-Schenk, S. and Agre, P. (1992) Mammalian red cell membrane Rh polypeptides are selectively palmitoylated subunits of a macromolecular complex. J. Biol. Chem. **267**, 5569–5574

48 Jayakumar, A., Schulman, I., Macneil, D. and Barnes, E. M. (1986) Role of the *Escherichia coli glnALG* operon in regulation of ammonium transport. J. Bacteriol. **166**, 281–284

49 Studier, F. W. and Moffatt, B. A. (1986) Use of bacteriophage T7 RNA polymerase to direct selective high-level expression of cloned genes. J. Mol. Biol. **189**, 113–130

50 Chang, A. C. and Cohen, S. N. (1978) Construction and characterization of amplifiable multicopy DNA cloning vehicles derived from the P15A cryptic miniplasmid. J. Bacteriol. **134**, 1141–1156

51 Wang, R. F. and Kushner, S. R. (1991) Construction of versatile low-copy-number vectors for cloning, sequencing and gene expression in *Escherichia coli*. Gene **100**, 195–199

Received 30 November 2001/15 February 2002; accepted 26 March 2002